

# Estimating the spatial and temporal distribution of snapping shrimp using a portable, broadband 3-dimensional acoustic array

Koay Teong Beng, Tan Eng Teck, Mandar Chitre, John R. Potter

Acoustic Research Laboratory, Tropical Marine Science Institute  
National University of Singapore, 12a Kent Ridge Road, Singapore 119223

[koay@arl.nus.edu.sg](mailto:koay@arl.nus.edu.sg), [ettan@arl.nus.edu.sg](mailto:ettan@arl.nus.edu.sg), [mandar@arl.nus.edu.sg](mailto:mandar@arl.nus.edu.sg), [johnp@arl.nus.edu.sg](mailto:johnp@arl.nus.edu.sg)

**Abstract - Broadband systems operating in warm shallow waters are often significantly affected by snapping shrimp (*Alpheus* & *Synalpheus*) that are reported to produce signals up to 300 kHz with source levels up to 190 dB re 1uPa @ 1m. Understanding the spatial and temporal distribution of these sources is crucial to their use either as insonifiers for Ambient Noise Imaging or to remove them as interfering noise for conventional sonar. The Acoustic Research Laboratory at the Tropical Marine Science Institute of Singapore has developed a high-bandwidth, compact 3-dimensional acoustic array that can localise these sources in time and space. It is a self-contained broadband system with four acoustic recording channels, each sampled at 500kSa/s. The main advantage of the system lies in its compact, portable size, permitting it to be easily deployed in open waters far off shore. The overall array size is about 1m with a cylindrical electronics housing of less than 230mm diameter and 600mm length. The system has been used to map high frequency noise sources within an area of some 20,000 m<sup>2</sup> from a single vantage point. An angular resolution of <1 degree has been achieved at the high end of the frequency range. The system has been deployed either as a surface-mounted (with spar buoy) or bottom-mounted (on a tripod) system with remote control capability over cable or as a stand-alone unit. The initial results show evidence of spatially clustered snapping. This paper presents the experimental results from deployments in 18-20m water depths among sparse reef patches approximately 1km offshore from the nearest islands and the estimated distribution of the snapping shrimp.**

## I. INTRODUCTION

Ambient noise in warm shallow waters is known to be dominated by bubble cavitations produced by snapping shrimp with a frequency range from 2kHz to more than 300kHz at levels reported up to 190dB re 1uPa @ 1m peak to peak level [1] [2]. These broadband ambient noises generally interfere with conventional sonar systems. However, the Acoustic Research Laboratory (ARL) at the Tropical Marine Science Institute, National University of Singapore has constructed a digital Ambient Noise Imaging

(ANI) camera that utilises these broadband ambient noise sources for acoustic imaging of totally silent objects [3] [4]. In support for this, the ARL conducted a series of local soundscape studies [5] that led to the development of a stochastic tomography inversion experiment to study the spatial and temporal distribution of snapping shrimp sounds [6] [7]. The experiment involved 6 units of 3-meter tall tripods that had to be positioned accurately on seabed to be able to produce distribution maps. In order to reduce the resources needed for such an experiment setup, the ARL subsequently developed a portable, high bandwidth acoustic data acquisition system [8] with a sensor array on a single tripod to replace the original 6-tripod setup.

## II. THE ACQUISITION SYSTEM

The acquisition hardware is a slightly modified version of our in-house developed portable broadband High Frequency Data Acquisition (HiFDAQ) system. The system simultaneously samples acoustic signals from 4 hydrophones at a high sampling rate up to aggregated 5MSa/s. It runs off an embedded Pentium processor that acquires data through a high speed PCI sampling card and writes the data into a 80GB Ultra-160 SCSI hard disk through a PCI-SCSI adaptor with a high-speed data bus of 160Mbps at maximum. The system is a battery operated self-contained submersible cylindrical electronics package with about 230 mm diameter and 600 mm length (excluding mounting fixtures). The four hydrophones are connected to the analogue signal conditioning board through underwater plugs using 4 to 5 meters of flexible thin cables. Modifications have been done to the system to increase its robustness and flexibility for this experiment.

The modified system includes an external watertight power on switch instead of an internal switch, avoiding having to open up the system on the field. All the internal system checks and calibrations are done only in dry laboratory. Both of

these reduce the salt crystal contamination to electronics.

The power supply module of the system has been upgraded to provide larger start-up current during system boot up. It is capable of providing 90W output power, 50% more than the power supply module of original system. A new industrial AC-DC power supply has been modified to provide an option to replace the battery pack when long-term operation is required and cable linkage is permitted. It accepts underwater AC power cable.

HiFDAQ has also been modified to accept an in-house customised underwater Ethernet cable (tested to 50m length). This opens up the option of remote acquisition control even when the system is in water. Such a configuration has been deployed in 18 meters water depth, about 30 meters away from a surface station.

The original HiFDAQ housing has been replaced with aluminium body after a heat dissipation issue was detected with its original PVC body. Certain electronics modules (especially the high speed acquisition module and the 10,000-rpm SCSI hard disk) in the system generate heat raising the system temperature to 50~60°C. The new aluminium cylinder provides much more efficient heat dissipation into the ocean, as it acts as a gigantic heat sink. The original end caps remain in use although they are made from plastics (since it is not in the main thermal path) but have been modified to accept new fittings for external switch and an underwater bulkhead for submersible Ethernet connection.

A mechanical clamp has been fabricated to firmly grip the housing body at one of its end while provides a coupling at the other. A series of fittings to the coupling have been manufactured to provide various mounting possibilities that allow the HiFDAQ to be deployed in various configurations. Fig. 1 shows the fully assembled electronics housing with the hydrophones and its new mounting couplings.

The four flexible hydrophones are fitted on a 3-dimensional array arranged in tetrahedron with 1-meter separation between each adjacent tip. An electronic compass with pitch and roll sensors has been installed on the tetrahedron frame in order to monitor its direction and levelling variation through out the entire acquisition period. Fig. 2 shows the tetrahedron frame with an underwater housing built specially to hold the electronics compass and level sensors on the frame.

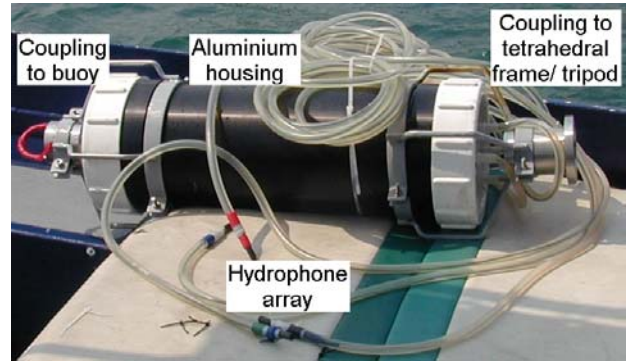


Fig. 1 Acquisition electronics package ready to be deployed.

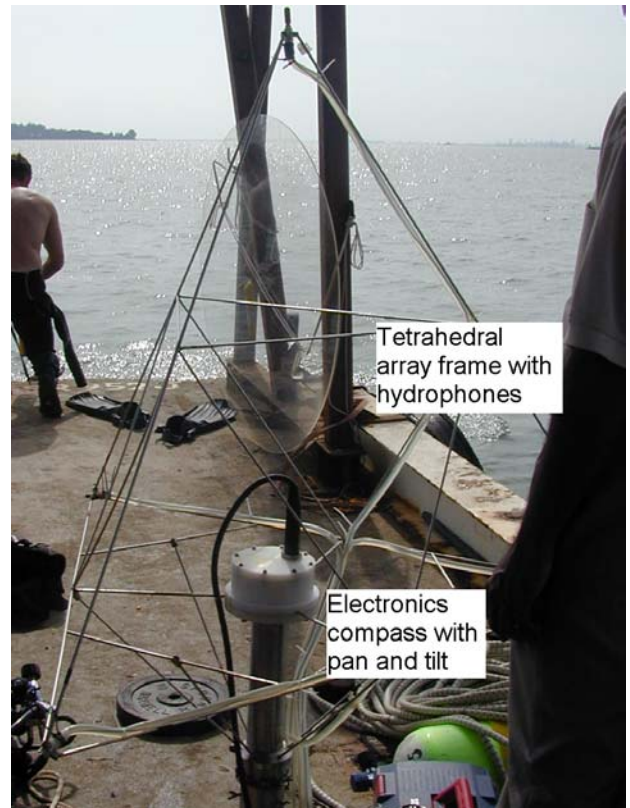


Fig. 2 Hydrophone array with orientation sensor waiting to be deployed, the white housing in the middle is the electronics compass and level sensors.

### III. EXPERIMENT SETUPS

The system, consisting of the HiFDAQ module and the tetrahedron module, can be deployed in various configurations depending on how the modules are mounted and coupled. It can be primarily deployed as surface mounted or bottom mounted system, each either in standalone mode or with a cable attached.

For the purpose of source distribution estimation, we have deployed the system in three different configurations. The first two configurations deployed the system from surface platforms, attached to either a buoy or the surface platform itself. For the first option, the tetrahedral frame was coupled directly to the electronics housing and the complete module was attached to custom-made flexible hose floatation that minimises vertical oscillation caused by the surface wave. This configuration ran in stand-alone mode and allowed us to deploy the system at open sea without a surface vessel in station. When the same physical setup was also deployed from a barge (or at times from surface vessels), it was secured from the surface by tensioned ropes, avoiding rotational oscillations. The tetrahedron frame was deployed in an inverted orientation in these two cases, typically 10 to 13 meter from seabed, as illustrated in Fig. 3(a).

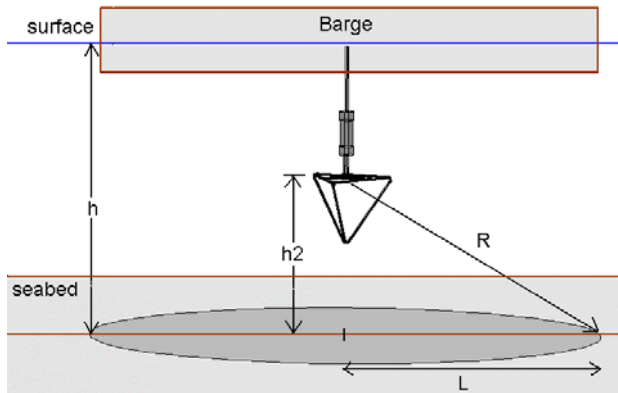


Fig. 3(a) HiFDAQ in surface mounted configuration.

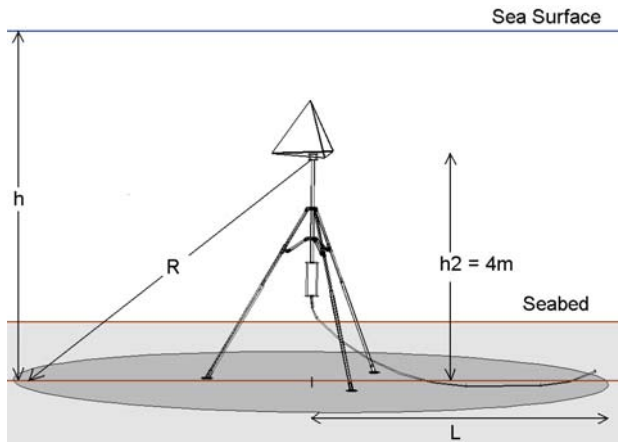


Fig. 3(b) HiFDAQ in bottom mounted configuration.

A number of deployments have also been done with bottom-mounted configuration, attached to a 4-meter tall tripod. The entire system is mounted on the seabed as shown in Fig. 3(b). The electronics

housing is attached at the lower end of vertical pole using the same coupling but different fittings; while the tetrahedron array frame is mounted on top, 4 meters above the seabed. With this, we are able to map more than 20,000m<sup>2</sup> of area centred at the tripod. The system was deployed for 24 hours in 18 to 20 meter water, recording data for 20 minutes approximately every 2 hours. Due to the intended long period acquisition, we powered and remotely controlled the system from a barge 30 meters away although the system can operate in a stand-alone mode (battery operated for up to 5 hours before it has to be recovered and recharged).

#### IV. ALGORITHM AND SIMULATION

The data collected from the deployments can be processed using an in-house developed algorithm. The algorithm finds the direction, in terms of azimuth and elevation angles, of the high frequency broadband transient signals within the data set by deterministically identifying individual clicks in each of the four channels and calculating propagation delays between them. The following section describes the algorithm and the associated geometry.

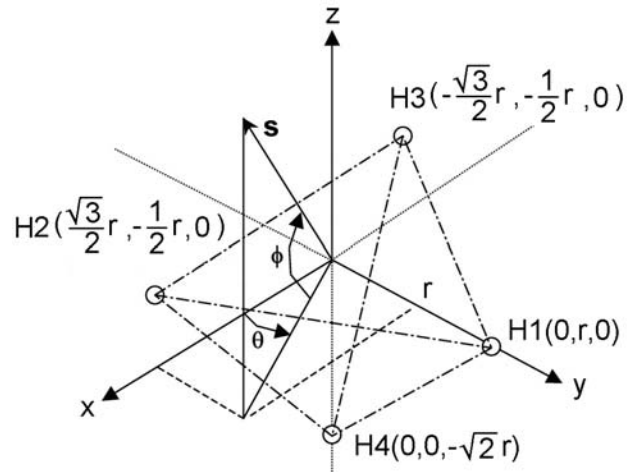


Fig. 4 Geometry setup of the tetrahedron array, with H1, H2 & H3 in the x-y plane and H4 lying below.

The frame of reference for the geometry of 3D sensor array is constructed with the origin at the centroid of the triangle forming the tetrahedron base and having the fourth hydrophone pointed in the negative z direction (see Fig 4). The positions of the four hydrophones (H1, H2, H3, H4) are then described in vectors space as  $\underline{h}_1$ ,  $\underline{h}_2$ ,  $\underline{h}_3$ , and  $\underline{h}_4$ . r is the distance between each of the sensors in the triangular base and the origin, and is related to tetrahedron arm length as

$$r = \frac{l}{\sqrt{3}},$$

where  $l$  the length of the tetrahedron arms (i.e. the distance between hydrophones), which is 1.2 m at current setup.

The incoming wave direction is described with a unit vector  $\underline{s}$  in Cartesian axis as shown in Fig. 4 and following expression.

$$\underline{s} = \begin{bmatrix} -\cos\theta \cos\phi \\ -\cos\phi \sin\theta \\ -\sin\theta \end{bmatrix},$$

The effective distance of each hydrophone from the origin, projected into the direction of incoming wave can be expressed as

$$d_i = \underline{h}_i \bullet \underline{s},$$

where  $i = 1, 2, 3, 4$  are the four hydrophones.

The travel delays between hydrophone H2, H3 and H4 with reference to hydrophone H1 can be written as

$$\begin{aligned} D_{j1} &= (d_j - d_1) \\ &= (\underline{h}_j - \underline{h}_1) \bullet \underline{s} \end{aligned}$$

where  $j = 2, 3, 4$  are the hydrophones.

The time lag in term of sampling interval is therefore

$$T_{j1} = \frac{fs}{c} [(\underline{h}_j - \underline{h}_1) \bullet \underline{s}]$$

$\underline{s}(x,y,z)$  is the unit vector of interest that is to be solved in term of  $x$ ,  $y$  and  $z$  axis (from which we obtain the  $\theta$  and  $\phi$  later), while  $T_{j1}$  can be obtained from the recorded time series after signal processing. The sampling frequency of each individual channel,  $fs$ , is set to 500kSa/s; while the sound velocity in the experiment site,  $c$ , is estimated to be 1540 m/s; giving us the sampling resolution of a about 3 mm. The rest of the terms in

the above expression are constants based on the geometry and system specifications.

With known angles  $\theta$ ,  $\phi$ , water depth  $h$ , height of array from seabed  $h_2$ , and assuming locally flat seabed and source to be located on the seabed, we estimate the ranges of each identified transient source from the array,  $R$ . We then correct the spreading loss for the range and estimate the source level of the transients. These sources are then mapped out in 2-dimensional space, within the radius of  $L$ , resulting in source distribution. The signal processing has been implemented using Matlab scripts and the above algorithm.

The algorithm assumes flat seabed and entire snapping shrimps population stays on seabed. Nevertheless, these might not be true in actual scenario in which the seabed might have some local variations, snapping shrimps might stay near to seabed instead of on it and the cavitation bubbles produced by the snapping shrimps could collapse at different heights off the seabed (although their height variations are small). The source level estimations might include errors introduced by range error ( $\delta R$ ) due to errors of sources height from seabed ( $\delta z$ ). Relation between  $\delta R$  and  $\delta z$  is related to height of array from seabed and horizontal distance source from array. For  $h_2 = 10m$  and  $L = 80m$  (surface mounted configuration),

$$\delta R = 10\delta z$$

For  $h_2 = 4m$  and  $L = 80m$  (bottom mounted configuration),

$$\delta R = 20\delta z$$

Therefore, the source level estimation error would not be more than -6dB when source is 100mm above the assumed ideal seabed at 80m away at the bottom mounted configuration.

A simple simulation verified the geometry, mathematics and the overall code functionality. The simulation was performed against a field of simulated snapping shrimp snaps and respective angular (3 dimensional direction) time lags for each of the four simulated hydrophone channels. A random noise of -26dB below signal was added to the signal on the hydrophones. Simulated snap distribution scenarios included a scenario with constant elevation angle and a full 360-degree azimuth placement of source snaps at 1-degree interval. The time series was then processed by the algorithm and a map of the source locations was generated. Extra clicks have been generated at  $\theta$

equals to 12 degrees, which was observed as red spot on the ring. The result is shown in Fig. 5.

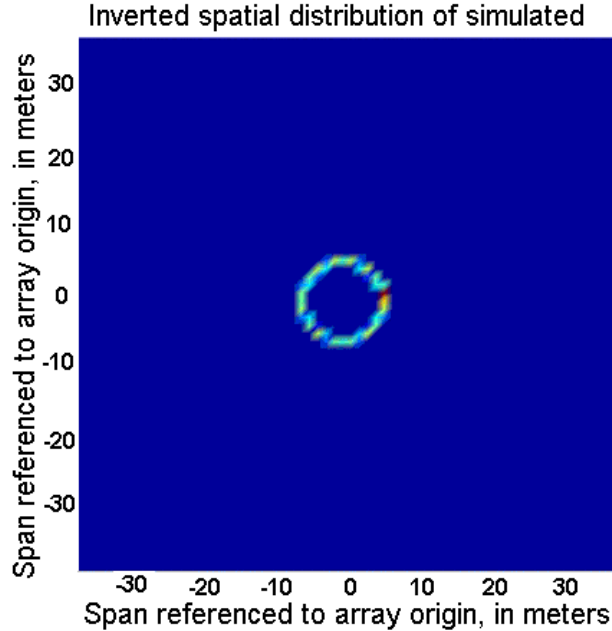


Fig. 5 Map produced from simulated sources distributed on seabed in a ring configuration

## V. EXPERIMENTAL RESULTS

This section presents some samples of data collected from two different sites. Site A is near a small island while site B is located within an anchorage area. The sites exhibit nominal depth of 15 to 18 meters at low tide, and are near sparse reef patches. Both data sets have been collected with the system deployed from barges stationed around the area. The sample data at site A was recorded at daytime around 13:15 ~ 13:35 while the sample data from site B was taken early in the morning between 2:40 ~ 3:00. The analysis presented here assumes that the sea floor is locally flat, although it has some bathymetric variations. The sound speed in water is estimated to be around 1540m/s and assumed to stay unchanged across the entire area under investigation during the data acquisition period.

### A. High frequency ambient noise directivity

Fig. 6 shows the azimuth directivity (over 360 degree at 1 degree interval) of ambient noise collected at site B. The energy directivity was derived by summing the high frequency source power (800Hz – 200kHz) over all elevation angles for each azimuth angles. This was done over all the clicks identified within the 20-minute data set, including the surface reflected clicks. The difference in total power from each direction is then plot in dB

scale with reference to the lowest energy level observed. The plot shows three directions where energy is substantially larger than the average. Source patches located in these directions are observed in the distribution maps shown later in this paper.

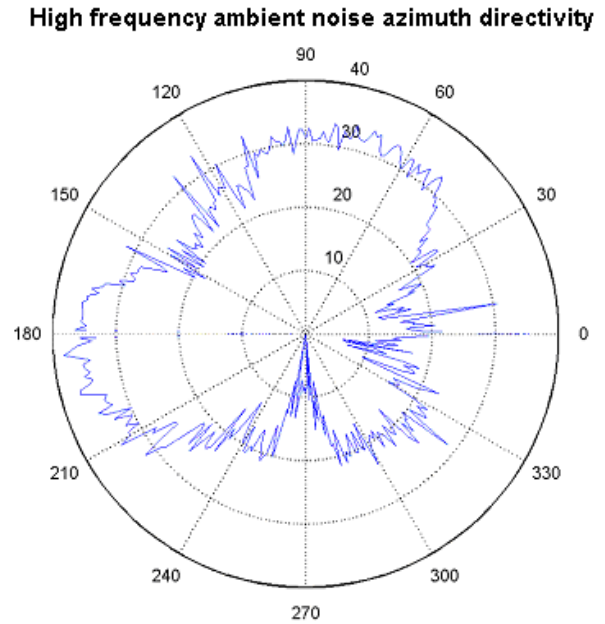


Fig. 6 Directivity plot of high frequency ambient noise at site B.

### B. Power Distribution Function of recorded time series

Next we investigated two 20 second long time series recorded on one of the hydrophones, selected from data sets recorded from each of the sites. Each of the raw time series was divided into 2048 sampling point (about 4.1ms length) windows, and then the average power in each window was calculated. The resulting probability density function (PDF) of power is shown in Fig 7.

The median of the distribution is at 126.4dB re  $1\mu\text{Pa}^2$  at site A and 121.2 dB re  $1\mu\text{Pa}^2$  at site B with standard deviation of 0.98 and 2.6 dB re  $1\mu\text{Pa}^2$  respectively. The observed lognormal probability distribution confirms the findings from acoustic recordings by Lim Tze Wei et al. in Singapore local water, which suggested a hypothesis that such lognormal distribution could be caused by noise sources that are either temporally random but spatially clustered or temporally chorusing but spatially homogeneous [2]. The PDF from site B data shows a small, local distribution “bump” at the high power end of the distribution that has low counts according to the global characteristic of the distribution (see Fig 7). This lognormal distribution suggests that source distribution in site B is more

likely to be spatially clustering rather than temporal chorusing.

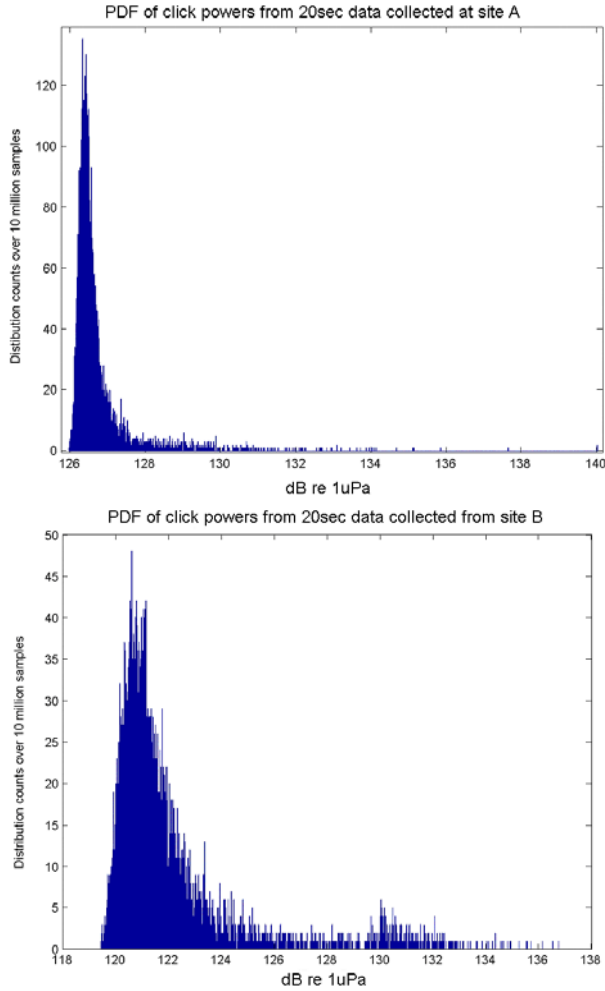


Fig. 7 Power Distribution Density of time series over 20 sec data (not range corrected)

**C. Spatial distribution of source snaps**

From the analysis of the acoustic power probability distributions, we move on to investigate the spatial distribution density of source snaps. The data collected from the four hydrophones was processed to identify individual snaps. The inter-channel time delays of a snap are mathematically inverted to resolve the direction of the snap and hence the source location on the seabed (assuming the sources are on seabed). The snap occurrence of each look angle (at about 1 degree angular resolution) is counted over 20 minutes and their peak to peak source levels are plotted in their respective source location in Cartesian as shown in Fig 8. Both sites presented different distribution patterns. The area under investigation was known to have sparse reef patches that could be associated with the distribution pattern.

Nevertheless, No ground truth operation has been carried out at the site so far to help explain these observed distributions. Site B's distribution is clearly seen to be correlated to the high frequency directivity shown previously in Fig 6. More field trials have been carried out in order to confirm the repeatability of the distribution.

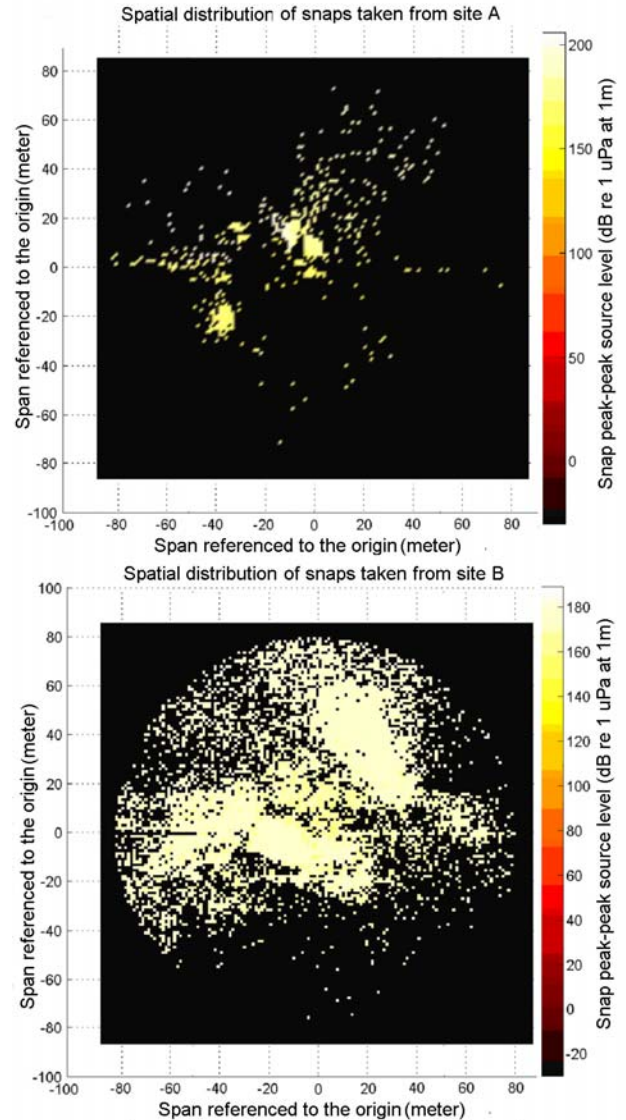


Fig. 8 Spatial distribution of mean snap power at source

The source level (SL) of each snap was calculated by taking into account the spherical spreading loss of  $20\log R$ , where R is the estimated range of each clicks to the centre of the array based on their directions calculated, assuming the shrimps are distributed on seabed. It is found that peak-to-peak source level is around 176.8 dB re  $1\mu\text{Pa}$  (standard deviation of 7.6 dB re  $1\mu\text{Pa}$ ) and 172.7 dB re  $1\mu\text{Pa}$  (standard deviation of 4.5dB re  $1\mu\text{Pa}$ )

for snaps recorded at site A and site B respectively. These levels may look smaller than previously reported levels, but we have crosschecked the levels with randomly sampled snapping shrimp sounds recorded from a recent ROMANIS recording. ROMANIS is an independent hardware system. Both systems reasonably agree with each other in terms of the observed source levels.

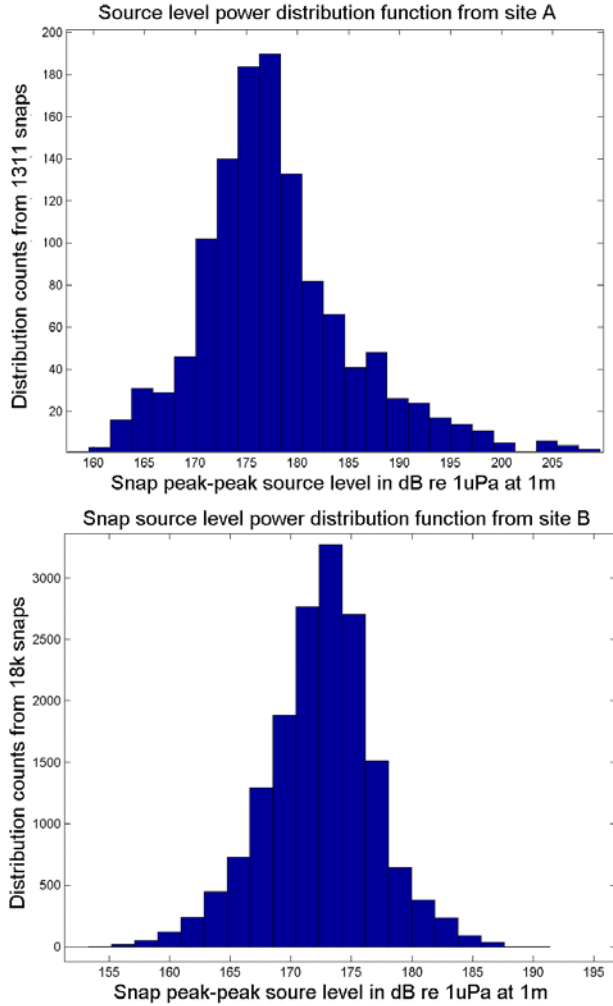


Fig. 11 Source level PDF shows mean snap power around 173 ~ 177 dB re 1  $\mu$ Pa at 1m

#### D. Temporal variation of snap power

Fig. 10 illustrates the peak-to-peak power of 1200 snaps occurred over time. Due to the large number of snaps, only 1200 individual snaps have been sampled from the entire raw time series. From about 19000 snaps identified by the algorithm, the 1200 sample is resulted from picking 1 snap in every 17 snaps. The graphs therefore represent the nominal snap powers over the entire 20 minute-time series. Snaps are plotted in their order of occurrences but the x-axis is not scaled in time, as the snap intervals are random. Fig 10 shows that

the snap power distribution has a reasonably constant median over the 20 minutes.

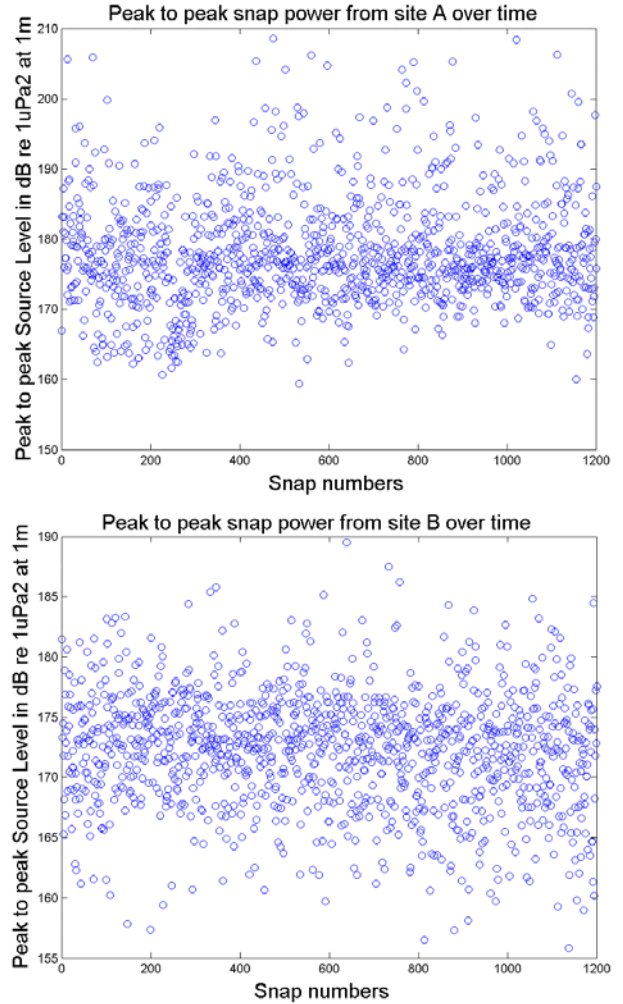


Fig. 10 Source levels of 1200 snaps samples from the 20 seconds data collected from both sites

## VI. CONCLUSIONS

The ARL has developed an easily deployable system for estimating spatial and temporal distribution of high frequency, broadband source mainly generated by snapping shrimp. The field results showed significant spatially clustered distributions in the observed areas. The source levels in the spatial distributions were estimated to be around 173 to 177 dB re 1 uPa @ 1m. The high frequency ambient noise directivity of the area has been estimated. And preliminary temporal distribution of the snapping shrimp click has been investigated. More trials have been conducted to confirm the repeatability of the observations.

The system has been successfully tested in field trials and has helped in localizing transient source locations. Such ambient noise source location

information is useful for other experiments undertaken in the same area such as the ROMANIS trials.

## REFERENCES

- [1] Au W.L. & Banks K., "The acoustics of the snapping shrimp *Synalpheus parneomeris* in Kaneohe Bay", pp41-47, *J. Acoust. Soc. Am.* **103** (1), 1998.
- [2] John R. Potter, Lim Tze Wei & Mandar Chitre, 'High-frequency ambient noise in warm shallow waters', *Sea Surface Sound*, UK 1997.
- [3] J. R. Potter, "Acoustic imaging using ambient noise: some theory and simulation results", *J.A.S.A.*, Vol. 95(1), 1994.
- [4] Venugopalan,P., Deshpande,P., Badiu,S, Constantin,S. , Lu, B. & Potter, J.R., "A 1.6 Gigabit/second, 25-85 kHz Acoustic Imaging Array- Novel Mechanical and Electronics Design Aspects", *OCEANS 99 MTS/IEEE Conference Proceedings*, Vol.1, Seattle, Sept 1999.
- [5] Potter J. R., Lim T. W. & Chitre M. A., "Ambient noise environments in shallow tropical seas and the implications for acoustic sensing", *Oceanology International* 97, Singapore, 1997.
- [6] Hong, L, Koay T. B., Potter, J.R. & Ong S.H., "Estimating snapping shrimp noise in warm shallow water", *Oceanology International '99*, Singapore 1999.
- [7] Potter J.R. and Koay T.B., "Do snapping shrimp chorus in time or cluster in space? Temporal-spatial studies of high-frequency ambient noise in Singapore waters", *European Conference on Underwater Acoustics 2000*, Lyons, France. July 2000.
- [8] Teong Beng; Koay Eng Teck Tan; Potter, J.R., "A portable, self-contained, 5msa/s data acquisition system for broadband, high frequency acoustic beamforming", *Oceans '02 MTS/IEEE*, Page(s): 369 – 378, Volume: 1, Oct. 29-31, 2002.